DOI 10.1007/s11106-016-9791-2
Powder Metallurgy and Metal Ceramics, Vol. 55, Nos. 3-4, July, 2016 (Russian Original Vol. 55, Nos. 3-4, March-April, 2016)

EFFECT OF CARBON CONTENT ON MICROSTRUCTURE AND MECHANICAL PROPERTIES OF POWDER METALLURGY STEELS

M. Turkmen[1]

UDC 621.762+669-1:661.872

In this study, steels, containing different proportions of C, were produced through powder metallurgy. The microstructure and mechanical properties of the produced powder-metallurgy (PM) steels were examined. The sintered density of PM steels was determined, and their microstructures were identified with optical microscopy, SEM, and EDS analyses. The results indicated that there was a significant increase in strength, but a decrease in elongation with an increase in C content. Considering the advantages of PM method, the results achieved in this study came almost close to rolled steel products.

Keywords: *powder metallurgy, steel, microstructure.*

INTRODUCTION

As it is known, there is a little bit of steel in everybody's life and it has many practical applications in several areas [1]. Steels represent the most important group of engineering materials as they have the widest diversity of applications compared to any other engineering materials [2, 3]. Steels continue to gain wide use as prospective functional and structural materials because of their good soft-magnetic properties, high strength, good corrosion, and wear resistance combined with relatively low material cost [4–6]. Steel is an alloy of iron and carbon. The steel is being divided into low carbon steel, high carbon steel, and medium carbon steel on the basis of carbon content. As the carbon content increases, the metal becomes harder and stronger but less ductile and more difficult to weld [7, 8].

Powder metallurgy (PM) processes provide economic as well as technical benefits over conventional processes using wrought materials, the advantages being cost reduction, improved performance, design flexibility, and the production of unique materials. The manufacturing processes for pressed and sintered PM parts consist of powder production, cold compaction, and finally sintering. Such parts are used in applications requiring low mechanical property levels [9–11]. Attraction and interest in net shape and near net shape manufacturing find PM to be a competitive method of manufacturing particular parts such as tool components in the mass production of machines [9, 12]. The major tonnage of metallic powders is being used as PM parts in numerous applications, parts for the automotive industry, for off-road construction equipment, gear pumps, outdoor garden equipment, and, recently, parts for space use, being some examples [9, 13]. PM process is a versatile and efficient route for producing components with combinations of various alloying elements. These alloying elements significantly

[1]Kocaeli University, Hereke Vocational School, Department of Metallurgy, Kocaeli-Hereke, Turkey; e-mail: mustafa.turkmen@kocaeli.edu.tr.

Published in Poroshkovaya Metallurgiya, Vol. 55, Nos. 3–4 (508), pp. 53–61, 2016. Original article submitted October 13, 2015.

improve the hardenability by shifting the transformation curves to the longer transformation time. Subsequent heat treatment results in enhancing the mechanical properties of the ferrous alloys [14–16].

In the literature, it has been seen that the production of steel is carried out through casting, rolling, and controlled cooling. In recent years, steel has also been produced with powder metallurgy method [12, 17, 18]. For example, R. Narayanasamy et al. [12] produced steels of the composition Fe–0% C, Fe–0.4% C, and Fe–0.8% C by using PM technique. In their studies, they carried out sintering operation in an electric muffle furnace at 1393 K. It was found that as the C content increased in the produced PM steel, the amount of perlite also increased, however pores magnitude decreased. In another study, Erden et al. [17] investigated the effects of Ti additions on the microstructures and mechanical properties of microalloyed powder metallurgy (PM) steels. For this purpose, Fe–0.25C, Fe–0.25C–0.1Ti, Fe–0.25C–0.15Ti, and Fe–0.25C–0.2 Ti powders were produced. Sintering of all samples was carried out in a tube furnace in a controlled argon atmosphere at 1423 K. Experimental results showed that Ti microalloyed steels can be produced by PM technology. The addition of Ti increases the strength in the sintered conditions. In addition, Ti limits grain growth during austenitization prior to cooling. By limiting austenite grain growth, the precipitates result in significant improvement in strength.

Schade et al. [19] investigated the effects of silicon and vanadium additions on the mechanical properties and microstructures of PM alloy. Samples for transverse rupture and tensile testing were compacted at a pressure of 690 MPa and then sintered at 1533 K for 30 min in an atmosphere of 90% nitrogen and 10% hydrogen. For heat treatment, samples were austenitized at 1173 K for 60 min in 75% nitrogen and 25% hydrogen atmosphere prior to quenching in oil. The quenched specimens were then tempered at 473 K for 1 h. It has been demonstrated that the addition of silicon and vanadium increased the strength in both the sintered and heat treated conditions.

The literature from previous works in the field of Fe–graphite powder metallurgy steels showed that no work had been carried out for determining the tensile test. Hence, this article mainly focuses on the study of tensile testing and also emphasizes on microstructure of Fe–graphite PM steels. For this purpose, graphite was added to several PM steels. Mechanical properties were measured and microstructures characterized in the sintered condition.

MATERIALS AND EXPERIMENTAL PROCEDURE

Iron and graphite powders were supplied by Högonas in mean particle sizes of 100 and 20 μm, respectively. Analysis indicated that the purity of Fe and graphite was 99.9 and 99.5%, respectively. The Fe–0.15 graphite (A1), Fe–0.25 graphite (A2), Fe–0.35 graphite (A3), Fe–0.45 graphite (A4), Fe–0.55 graphite (A5), and Fe–0.65 graphite (A6) powders were prepared by mixing for 1 h in an industrial conic mixer. Zinc-stearate was also used in all mixes as lubricant. Tensile test specimens were compacted uniaxially at a pressure of 700 MPa using a hydraulic press of 100 t capacity. The test pieces were sintered in a high-temperature tube furnace in a controlled argon atmosphere. The sintering process applied to the test specimens involves heating to 1423 K at a rate of 278 K/min, holding at this temperature for 1 h, and cooling to room temperature at a rate of 278 K/min. Prior to mechanical testing, green and sintered density values were obtained through water displacement Archimedes method.

Tensile test was carried out at room temperature using a Schimadzu tensile testing machine at a crosshead speed of 1 mm/min. Triplicate samples were employed per run in order to correct for minor differences in experimental conditions. Figure 1 shows the tensile test specimen used in this study.

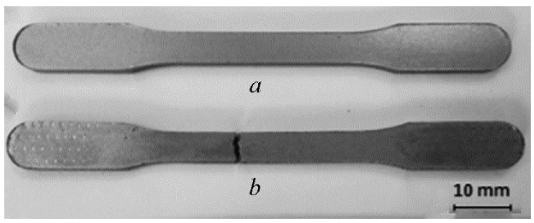

Fig. 1. General view of the tensile test specimen sintered at 1150°C for 1 h: (*a*) before and (*b*) after fracture

The examination of steel microstructures was carried out using an optical and scanning electron microscope (SEM). Energy dispersive spectrometry (EDS) was used to provide elemental analysis on precipitate particles. Specimens for microstructural characterization were prepared using standard metallographic procedures. Etching times were closely monitored to prevent overetching of the alloys due to the fineness of their microstructure. The microstructures were examined with a Nikon Eclipsel L150 type microscope capable of magnifications between 50× and 1000×. The phase volume fraction measurement was also carried out using a Clemex Vision Lite type image analysis system.

RESULTS AND DISCUSSION

The variation in mechanical properties in PM steel and microalloyed PM steels can be explained in terms of microstructure obtained by cooling after sintering. Figure 2 shows the evaluation of the microstructure for Fe–0.15 graphite (A1), Fe–0.25 graphite (A2), Fe–0.35 graphite (A3), Fe–0.45 graphite (A4), Fe–0.55 graphite (A5), and Fe–0.65 graphite (A6) PM steels under sintered conditions. It is seen that optical microstructure of the PM steels consists of ferrite and pearlite structure in different volume fractions depending on graphite amount.

Table 1 also shows the relative and green density, porosity, and phase volume fractions under sintered conditions. As can be seen, a sharp increase in the pearlite volume fraction of the PM steels was observed with increasing graphite content. For example, the addition of graphite in the percentage of 0.1, 0.25, 0.35, 0.45, 0.55, or 0.65 led to an increase in pearlite content to 2, 7, 17, 22, 36, and 45%, respectively. These results are consistent with the results obtained by Güral and Tekeli [20]. It was also observed in Fig. 2 that there were partially unclosed pores on grain boundaries of produced PM steels. Although the pores negatively affect strength, small pores with a spherical shape do not decrease strength [21, 22].

Table 2 illustrates the mechanical properties of PM steels by showing yield strength (YS), ultimate tensile strength (UTS), and percentage elongation. Figure 3 also shows typical examples of the stress–strain curves obtained from the tensile tests. It can be seen from Table 2 and Fig. 3 that yield strength and tensile strength of PM steels increase with increase in graphite content to 0.15, 0.25, 0.35, 0.45, 0.55, or 0.65 (wt.%). Elongation tends to decrease with increasing graphite content. These changes would be expected as a result of the differences in grain sizes and pearlite amount. Gündüz and Çapar [23] studied the influence of forging and cooling rate on microstructure and properties of medium carbon microalloyed forging steels. They showed that higher strength

TABLE 1. Relative and Green Density, Porosity, and Volume Fractions of Pearlite Phases in PM Steels

Alloy	Green density, %	Relative density, %	Porosity, %	Pearlite, %
1	89	94	6	2
2	88	93	6	7
3	87	93	7	17
4	88	93	7	22
5	86	92	8	36
6	88	92	8	45

TABLE 2. Mechanical Properties of Sintered PM Steels

Alloy	YS, MPa	UTS, MPa	Elongation, %
1	103	210	19
2	112	224	15
3	119	229	14
4	144	252	13
5	175	322	10
6	248	376	9

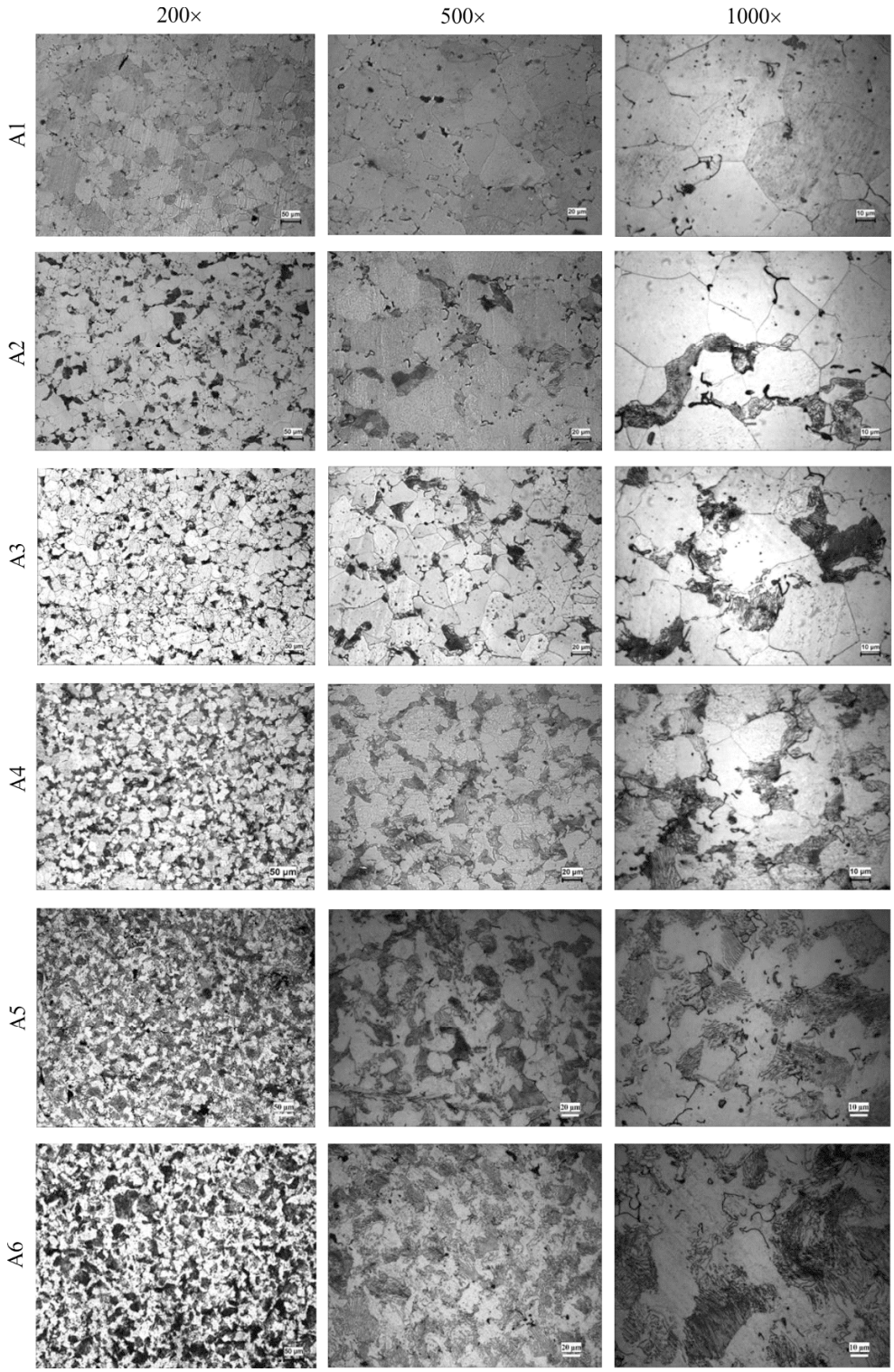

Fig. 2. Microstructures of sintered PM steels: (A1) Alloy 1, (A2) Alloy 2, (A3) Alloy 3, (A4) Alloy 4, (A5) Alloy 5, and (A6) Alloy 6

combined with adequate elongation to fracture was achieved in steels due to the finer grain sizes and larger pearlite contribution.

The density is also expected to significantly affect properties of PM steels because residual porosity reduces strength. The interparticle voids in the loose powder cannot be completely eliminated by uniaxial cold

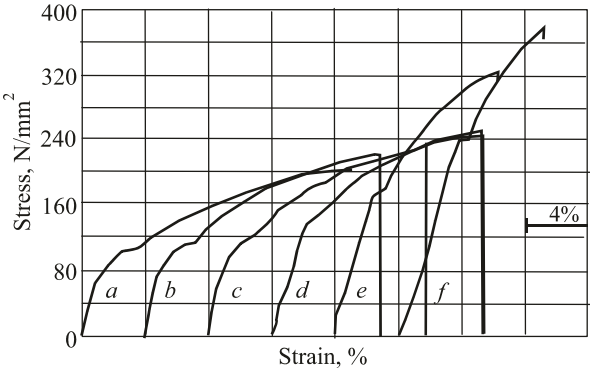

Fig. 3. Variation of stress–strain curves of PM steels with different percentage of graphite contents: Alloys 1 (*a*), 2 (*b*), 3 (*c*), 4 (*d*), 5 (*e*), and 6 (*f*)

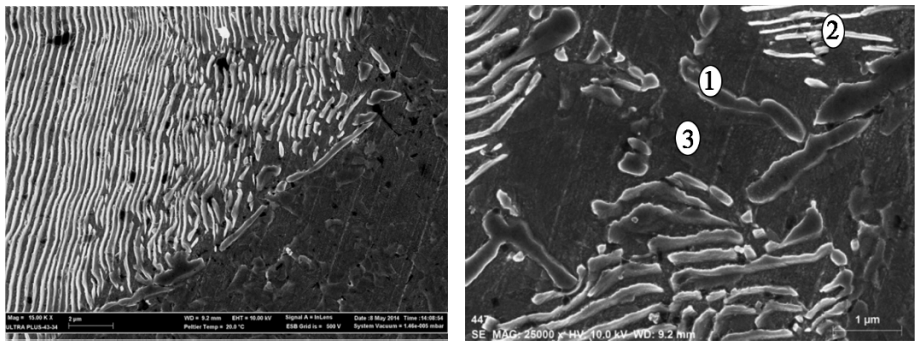

a *b*

Fig. 4. SEM images for Alloy 4: (*a*) low magnification, (*b*) high magnification and indicated EDS points in Alloy 4

TABLE 3. EDS Results for Indicated Points in Alloy 4 (See Fig. 4 for Points)

Spectrum, at.%	Composition, at.%		
	C	N	Fe
1	22.18	1.48	76.34
2	13.37	1.46	85.17
3	18.45	1.44	80.12

compaction, and sintering shrinkage, if present, cannot lead to full density. The final density of most steel parts produced using this technology ranges between 6.9 and 7.2 g/cm^3, which corresponds to a fractional porosity of 0.11 and 0.06, respectively (assuming a theoretical density of 7.7 g/cm^3) [24]. In the present experimental work, PM steels showed similar relative density, i.e., 92 and 94% for the as-sintered condition. This may explain that an increase in strength is due to the presence of different pearlite amounts.

Figure 4 shows SEM images and EDS analysis at points 1, 2, and 3 marked on the microstructure of Alloy 4 (Fe–0.45 graphite). Table 3 shows EDS results of the indicated points in Alloy 4. It is seen from Table 3 that points 1, 2, and 3 have Fe and C contents. The presence of these elements indicates that Fe_3C appeared during sintering and/or after sintering. The majority of the matrix is a very Fe-rich phase with slightly elevated C concentration.

PM steels were analyzed using XRF technique to determine their elemental compositions. The sample preparation for XRF is relatively simple as it requires less time and effort. For example, when a solid sample is

homogeneous, it needs only polishing to be ready for analysis [25]. The chemical composition (in wt.%) of Alloy 4 (Fe–0.45 graphite) is presented below:

Fe	C	Si	Mn	P	S	Cr	Ni	Al
99.23	0.249	0.005	0.211	0.009	0.016	0.082	0.046	0.044

It can be noted, that most elemental compositions obtained conform to the values claimed by PM steels.

Fractographic studies of the tensile test specimens were carried out by SEM. Figure 5 shows the fracture surfaces of Alloy 1 and Alloy 6. Changes were observed in the fracture with respect to the size, shape, and depth of the microvoids. It was seen from the fractograph of Alloy 1 (Fig. 5*a*) that the mode of fracture is purely ductile. This is evident from the presence of numerous dimples along with fine and rounded pores. It was generally apparent that the mechanism of fracture is void formation and coalescence. However, Alloy 6 (Fig 5*b*) showed dimples and cleavage facets indicating that the fracture is of mixed type. Large voids were also observed in the Alloy. These

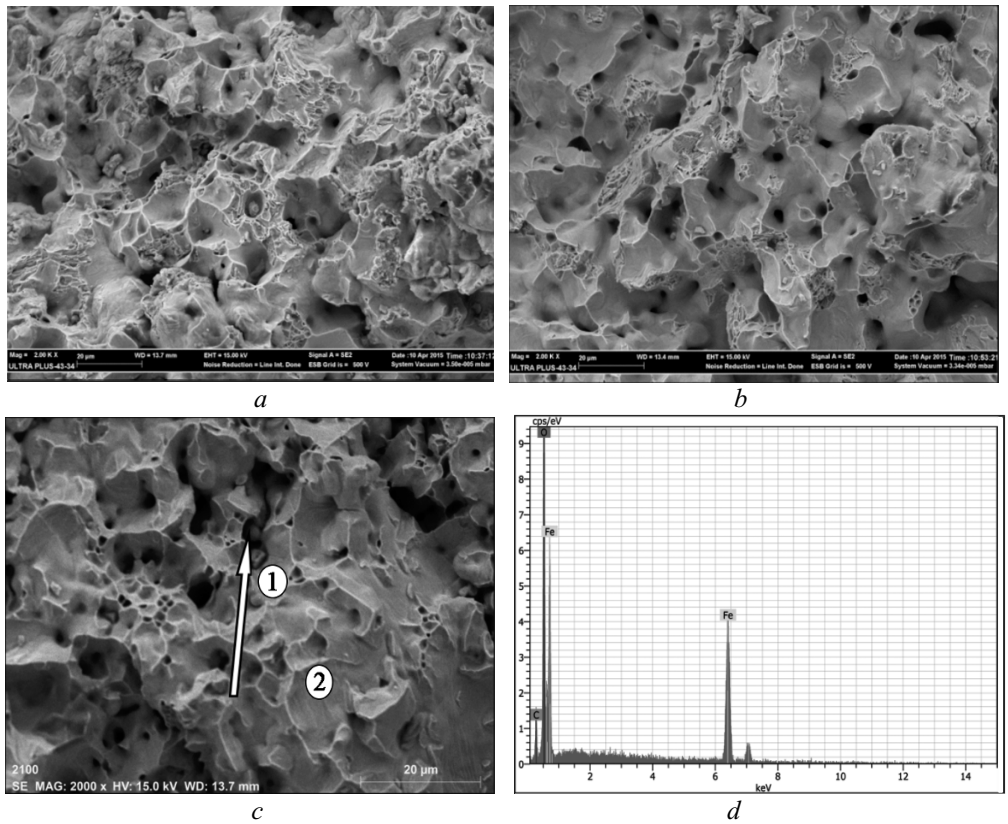

Fig. 5. Fracture surfaces of (*a*) Alloy 1, and (*b*) Alloy 6; (*c*) high magnification and indicated EDS points of in Alloy 6, (*d*) EDS charts from indicated particle of Alloy 6

TABLE 4. EDS Results for Indicated Points in Alloy 6 (See Fig. 5 for Points)

Spectrum	Composition, at.%		
	C	O	Fe
1	8.67	31.64	59.69
2	1.51	–	98.49

voids are indicative of the removal of Fe_3C particulates through pulling of under heavy tensile loading conditions. The Fe–C–O-based particle inside the large microvoids of PM steel is clearly shown in SEM fractograph (Fig. 5*c* and 5*d*) and by corresponding EDS results in Table 4.

Erden et al. [17] investigated tensile behavior of sinter-forged Ti alloyed PM steel. They observed mixed (ductile-brittle) type of fracture in the microalloyed PM steel with Ti due to the formation of carbides and the carbide pull-off during heavy deformation.

CONCLUSIONS

Addition of graphite in different proportions to iron powder has no influence on densification of sintered PM steels. However, an increase in graphite content has shown higher rates of strength. However, the ductility of PM steels is found to decrease with the increase in the amount of graphite.

The fracture surface analysis showed that Fe–0.15C PM steel with a ferritic and pearlitic microstructure exhibits pure ductile fracture under tensile loading conditions. In the case of the Fe–0.65C PM steel, the mode of fracture is ductile and brittle giving a mixed fracture. The mode of fracture turned from ductile to ductile-brittle with the increase in carbon content.

REFERENCES

1. J. P. Sharma, S. Chaturvedi, and P. Arora, "Studies on effect of percentage of carbon on the tensile and compressive strength of structural steel," *Int. J. Eng. Sci. Technol.*, **4**, No. 5, 2328–2333 (2012).
2. M. S. Htun, S. T. Kyaw, and K. T. Lwin, "Effect of heat treatment on microstructures and mechanical properties of spring steel," *J. Met. Mater. Miner.*, **18**, No. 2, 191–192 (2008).
3. S. A. Tukur, M. M. Usman, I. Muhammad, et al., "Effect of tempering temperature on mechanical properties of medium carbon steel," *Int. J. Eng. Trends Technol.*, **9**, No. 15, 798–800 (2014).
4. A. Calik, A. Duzgun, O. Sahin, et al., "Effect of carbon content on the mechanical properties of medium carbon steels," *Verlag der Zeitschrift für Naturforschung*, **65**, 468–472 (2010).
5. A. Güral, S. Tekeli, D. Özyürek, et al., "Effect of repeated quenching heat treatment on microstructure and dry sliding wear behavior of low carbon PM steel," *Mater. Sci. Forum*, **534**, 673–676 (2007). DOI:10.4028/www.scientific.net/MSF.534-536.673.
6. S. Tekeli, A. Güral, and D. Özyürek, "Microstructure and dry sliding wear properties of 3Si–2Ni and 3Si–2Mn powder metallurgy steels with different graphite content," *J. Eng. Tribol.*, **225**, No. 8, 814–820 (2011). DOI:10.1177/1350650111405255.
7. S. R. Nimbhorkar and B. D. Deshmukh, "Effect of case hardening treatment on the structure and properties of automobile gears," *Int. J. Mod. Eng. Res.*, **3**, No. 2, 637–641 (2013).
8. D. O. Oluyemia, O. I. Oluwoleb, and B. O. Adewuy, "Studies of the properties of heat treated rolled medium carbon steel," *Mater. Res.*, **14**, No. 2, 135–141 (2011). DOI: 10.1590/S1516-14392011005000040.
9. P. W. Lee, in: E. Klar (ed.), *Powder Metallurgy Applications, Advantages and Limitations*, ASM, New York (1983).
10. T. K. Kandavel, R. Chandramouli, and D. Shanmugasundaram, "Experimental study of the plastic deformation and densification behavior of some sintered low alloy P/M steels," *Mater. Des.*, **30,** No. 5, 1768–1776 (2009). DOI: 10.1016/j.matdes.2008.07.027.
11. W. D. W. Angel, L. T. Jurado, E. C. Martinez, et al., "Effect of carbon on the density, microstructure and hardness of alloys formed by mechanical alloying," *Mater. Des.*, **60**, 605–611 (2014). DOI:10.1016/j.matdes.2014.04.039.
12. R. Narayanasamy, V. Anandakrishnan, and K. S. Pandey, "Effect of carbon content on workability of powder metallurgy steels," *Mater. Sci. Eng. A*, **494**, 337–342 (2008). DOI:10.1016/j.msea.2008.04.022.
13. M. Abdel-Rahman and M. N. El-Sheikh, "Workability in forging of powder metallurgy compacts," *J. Mater. Process. Technol.*, **54**, 97–102 (1995). DOI:10.1016/0924-0136(95)01926-X.

14. L. E. G. Cambronero, C. Fernandez, J. M. Torralba, et al., "Influence of powders on final properties and microstructure of sintered molybdenum steels," *Powder Metall.*, **37**, 53–56 (1994). DOI: http://dx.doi.org/10.1179/pom.1994.37.1.53.
15. M. Fodor and J. V. Wood, "Effect of carbon on microstructure of mixed powder system cooled at moderate rates after sintering," *Powder Metall.*, **38,** 141–146 (1995). DOI: http://dx.doi.org/10.1179/pom.1995.38.2.141
16. M. Youseffi, C. S. Wright, and F. M. Jeyacheya, "Effect of carbon content, sintering temperature, density, and cooling rate upon properties of prealloyed Fe–1.5Mo powder," *Powder Metall.*, **43**, 270–274 (2000). DOI: http://dx.doi.org/10.1179/003258900666041.
17. M. A. Erden, S. Gündüz, M. Türkmen, et al., "Microstructural characterization and mechanical properties of microalloyed powder metallurgy steels," *Mater. Sci. Eng. A*, **616**, 201–206 (2014). DOI:10.1016/j.msea.2014.08.026.
18. C. Schade, T. Murphy, A. Lawley, et al., "Microstructure and mechanical properties of microalloyed PM steels," *Int. J. Powder Metall.*, **48**, 51–59 (2012).
19. C. Schade, T. Murphy, A. Lawley, et al., "Microstructure and mechanical properties of PM steels alloyed with silicon and 3-vanadium," *Int. J. Powder Metall.*, **48**, 41–48 (2012).
20. A. Güral and S. Tekeli, "Microstructural characterization of intercritically annealed low alloy PM steels," *Mater. Des.*, **28**, 1224–1230 (2007). DOI:10.1016/j.matdes.2006.01.007.
21. W. Jing, W. Yisan, and D. Yichao, "Production of (Ti, V) C reinforced Fe matrix composites," *Mater. Sci. Eng. A*, **454**, 75–79 (2007). DOI: 10.1016/j.msea.2006.11.024.
22. S. Saritaş, M. Türker, and N. Durlu, *Powder Metallurgy and Particulate Materials Processing*, Turkish PM Publications (2007), pp. 404–410.
23. S. Gündüz and A. Çapar, "Influence of forging and cooling rate on microstructure and properties of medium carbon microalloy forging steel," *J. Mater. Sci. Lett.*, **14**, No. 2, 561–564 (2006). DOI: 10.1007/s10853-005-4239-y.
24. G. Cipolloni, C. Menapace, I. Cristofolini, et al., "A quantitative characterization of porosity in a Cr–Mo sintered steel using image analysis," *Mater. Charact.*, **94**, 58–68 (2014). DOI :10.1016/j.matchar.2014.05.005.
25. A. B. Blank and L. P. Eksperiandova, "Specimen preparation in X-ray fluorescence analysis of materials and natural objects," *X-Ray Spectrom.*, **27**, No. 3, 147–160 (1998). DOI: 10.1002/(SICI)1097-4539(199805/06)27:33.0.CO;2-P.